operation has been derived. For four-dimensional operations involving a pair of identical rotations two, and only two, of the expected four orientational parameters are free parameters. This confirms what has hitherto been believed but not proven.

References

WEIGEL, D., VEYSSEYRE, R., PHAN, T., EFFANTIN, J. M. & BILLIET, Y. (1984). *Acta Cryst.* A**40**, 323-330.
WHITTAKER, E. J. W. (1984). *Acta Cryst.* A**40**, 58-66.
WHITTAKER, E. J. W. (1985). *An Atlas of Hyperstereograms of the Four-Dimensional Crystal Classes.* Oxford: Clarendon Press.
WHITTAKER, E. J. W. (1990). *Acta Cryst.* A**46**, 940-942.

Acta Cryst. (1992). A**48**, 225-231

Interference of X-ray Diffraction Trajectories in a Strained Crystal Undergoing Ultrasonic Excitation

BY E. ZOLOTOYABKO

Department of Materials Engineering, Technion-Israel Institute of Technology, Haifa 32000, *Israel*

AND V. PANOV

Institute of Nuclear Problems, Belorussian State University, Lenin prospect 4, *Minsk* 220080, *USSR*

(*Received* 11 *March* 1991; *accepted* 13 *September* 1991)

Abstract

The X-ray optics in a strained single crystal under ultrasonic excitation are considered. The anomalous behavior of diffraction intensity, depending on sound amplitude, is analyzed. The interference of X-rays moving along different trajectories is demonstrated, which leads to a new type of *Pendellösung* effect, depending on the strain gradient and sound frequency. Experimental data agree with the theoretical predictions.

1. Introduction

The problem of ultrasonic influence on X-ray and neutron diffraction is now under intensive investigation. The most interesting phenomena arise when the magnitude of the ultrasound wave vector k is of the order of the gap Δk_0 between the branches of the dispersion surface (DS) (in the two-beam approximation). In this case diffraction is of a multiwave nature, since, together with the nodes 0 and H of the reciprocal lattice, the points $\pm mk$ and $H \pm mk$ will be located near the Ewald sphere (Entin, 1979). Formally, if

$$k > \Delta k_0 \qquad (1)$$

one speaks about the creation of an ultrasonic superlattice, which strongly modifies the eigenstates of diffracted quanta inside the crystal. Such ultrasound we will call here a high-frequency wave.

Interaction between modified Bloch states by means of high-frequency ultrasonic perturbation leads to new physical effects, such as the resonant ultrasonic suppression of the Borrmann transmission (Entin, 1977), the ultrasound-induced *Pendellösung* beatings in diffraction intensity (Iolin, Zolotoyabko, Raitman, Kuvaldin & Gavrilov, 1986; Entin & Puchkova, 1984) and anomalous behavior of diffraction intensity in elastically deformed crystals in the presence of acoustic waves (Iolin, Raitman, Kuvaldin & Zolotoyabko, 1988).

The latter effect consists of a substantial decrease (up to 50%) in the diffraction intensity I at small sound amplitudes w ($Hw < 1$, where H is the magnitude of the reciprocal-lattice vector), in contrast to the intensity growth in a thin nondistorted crystal undergoing ultrasonic excitation. Such curves were first obtained in a neutron diffraction experiment and were theoretically explained by E. Iolin in terms of the violation of the adiabaticity condition for quanta movement, taking into account the inelastic multiphonon scattering (Iolin, 1987).

Moreover, an additional *Pendellösung* effect was predicted, due to the interference of waves travelling along different trajectories inside the distorted crystal under ultrasonic excitation. In contrast with the well known results for elastically strained crystals without ultrasound (Kato, 1964; Hart, 1966), the new *Pendellösung* effect reveals itself in the form of diffraction intensity oscillations, measured at definite sound amplitudes. The oscillation period depends on the strain gradient b and sound frequency ν (more precisely on the parameter $k/\Delta k_0$). Preliminary results in this field, obtained with both X-ray and neutron beams, were reported at the Twelfth European Crystallographic Meeting (Iolin, Zolotoyabko, Raitman & Kuvaldin, 1989).

Here we present the detailed data concerning X-ray diffraction in elastically strained crystals undergoing high-frequency ultrasound.

0108-7673/92/020225-07$03.00

2. Theoretical considerations

The most suitable description of dynamic scattering is achieved in terms of an isoenergetic DS for the quanta traveling inside the crystal when the diffraction condition is obeyed. In the two-beam approximation there is the well known hyperbolic two-branch DS (see Fig. 1*a*) with a typical gap $\Delta k_0 = 2\pi/\tau$ (τ is the extinction length) which completely determines the diffraction pattern. The points on the DS (called tie points or dispersion points) correspond to the different X-ray incident angles in the vicinity of the Bragg angle Θ_B. In the case of a distorted crystal the description is in principle more complicated, since each place in the sample has its own DS. If strains are sufficiently smooth, with the strain gradient b satisfying the condition

$$B<1; \quad B=2Hb/\Delta k_0^2 \tag{2}$$

the quanta (X-ray or neutrons) move inside the crystal, 'tuning' adiabatically to the local DS without interbranch transitions. As has been shown (Penning & Polder, 1961), even in such a situation the diffraction process can be described in the framework of a single DS. However, the tie points, which are stationary for the undeformed lattice, will now move along DS branches in the directions indicated by the arrows in Fig. 1(*a*), as quanta penetrate into the crystal. It should be emphasized that x projections of point velocities (parallel to the crystal surface) have the same sign and magnitude for both DS branches. In such a representation it is easy to understand the growth of the diffraction intensity I_d (without the ultrasound) in a thin ($\mu T<1$, where μ is the linear X-ray absorption coefficient, T is the crystal thickness) distorted crystal in comparison with a perfect one, I_0.

Let us consider the state 1 (see Fig. 1*a*), which is excited near the entrance sample surface and does not give a contribution to the diffraction intensity in the case of a perfect crystal, because its group velocity

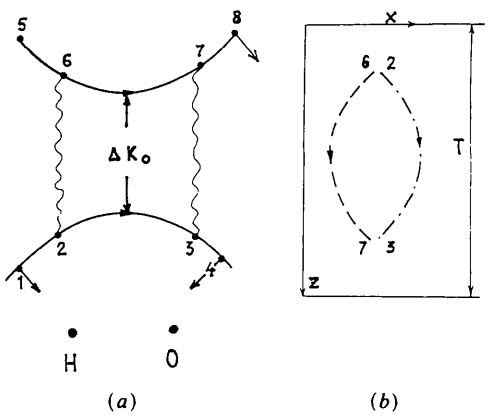

Fig. 1. Quanta movement in a strained crystal: (*a*) in momentum space along one dispersion surface; (*b*) in real space.

(normal to the DS) is nearly parallel to the direction of the incident beam (*i.e.* directed to the 0 node of the reciprocal lattice). For the elastically strained crystal (for example, with curved atomic planes) the tie point 1 moves under the strain gradient b along the DS branch and under definite conditions transforms into state 4, which already gives a contribution to the diffraction intensity, since its group velocity is parallel to the direction of the diffracted beam (*i.e.* directed to the H node). The ultrasonic influence in such a scheme consists in general of the transition stimulation between DS branches.

Actually, an incident wave excites the states 1 and 8 on the DS. In the absence of ultrasound point 1 moves along the trajectory 1-2-3-4 (see Fig. 1) and, as mentioned previously, transforms to state 4 corresponding to a diffracted wave. The direction of the movement of point 8 is such that it never gives a contribution to the diffraction intensity. Now consider a 'switch on' of high-frequency ultrasound with $k > \Delta k_0$. Such ultrasound mixes by a resonance process the Bloch states on the different DS branches, separated by the sound wave vector k, *i.e.* states, corresponding to the points 2,6 and 3,7 in Fig. 1. [Due to the real structure of X-ray wave functions the mixing effectively takes place only for transverse acoustic waves (Iolin & Entin, 1983).]

In spite of this, the movement of point 8 is not disturbed and its contribution to the diffraction intensity is again close to zero. The situation is changed drastically for point 1. Now, to go to state 4 it can move along two trajectories: (*a*) 1-2-6-7-3-4 and (*b*) 1-2-3-4.

At the transition point the tie point has the probability R_1 of remaining on the same DS branch and the probability M_1 of going over to the other one ($R_1+M_1=1$). Then for the (*a*) process one has a probability M_1^2 and for the (*b*) process R_1^2. Thus the intensity change ΔI at the expense of ultrasound is given by

$$\Delta I/I_d = (I-I_d)/I_d = I/I_d - 1 = R_1^2 + M_1^2 - 1$$
$$= -2M_1R_1 \le 0. \tag{3}$$

It follows from (3) that ultrasound can decrease the diffraction intensity by 50% ($M_1 = R_1 = \frac{1}{2}$). These qualitative considerations are very successful for understanding the nature of ultrasound influence on the diffraction intensity. The correct mathematical solution has been published (Iolin, 1987; Iolin, Raitman, Kuvaldin & Zolotoyabko, 1988), as have expressions for the probabilities R_1 and M_1, *viz*

$$R_1 = \exp[-\pi(Hw)/(2B)^{1/2}]; \quad M_1 = 1-R_1. \tag{4}$$

By differentiating (3) and taking into account (4), one finds the sound amplitude $w_{\min}$ corresponding to the minimum of the function $\Delta I/I_d$

$$(Hw)_{\min} = [(2B)^{1/2}/\pi] \ln 2. \tag{5}$$

Therefore, the diffraction intensity is essentially influenced by the weak acoustic wave with the amplitude under condition $(Hw)^2 \sim B < 1$. The decrease of diffraction intensity is explained by the process 1-2-7-8, *i.e.* interbranch scattering.

It is known, however, that such a situation can be realized without ultrasound at large strain gradients where $B \geq 1$. In this case the interbranch scattering leads to the restriction of diffraction intensity I by the kinematical limit I_∞. The probability of the percolation through the 'potential barrier' Δk_0 in the quasi-classical approximation is defined by the factor $f = \exp(-\pi/2B)$ (Chukhovskii & Petrashen, 1977; Lukas & Kulda, 1989).

From the physical point of view the interbranch scattering plays an essential role when the relative strain δ on the reduced extinction length, $\tau/2\pi$, exceeds the angular half width of the diffraction peak, $\Delta\Theta_0/2$:

$$\delta = b\tau/2\pi \geq \Delta\Theta_0/2 = \Delta k_0/2H. \qquad (6)$$

The condition $B \geq 1$ immediately follows from (6), using the B definition [see (2)].

As was previously mentioned, the probability of the sound-induced interbranch transition depends on the factor $\exp[-\pi Hw/(2B)^{1/2}]$. This arises because of angular satellites on the diffraction curve with width $\Delta\Theta_s = (\Delta k_0/H)Hw$ (Kohler, Mohling & Peibst, 1974; Entin, 1979). Additionally, such satellites create a new extinction length $\tau_s = \tau/Hw$ inside the crystal. Correspondingly, the condition (6) should be rewritten in the form

$$\delta = b\tau_s/2\pi \geq \Delta\Theta_s/2. \qquad (7)$$

From (7) it follows that the significant role of the small sound amplitudes is of the order $(Hw)^2 \simeq B$.

At $(Hw)^2 \gg B$, factor $M_1 \simeq 1$ and due to the intense reverse transition (7→3) the diffraction intensity is restored to the initial value. The action of one-phonon scattering is suppressed. Taking into account multiphonon scattering (Iolin, 1987), one obtains the dependence of the diffraction intensity on the sound amplitude in the shape shown in Fig. 2. We call it anomalous since, at small w, a decrease in $I(w)$ takes place. Further, at increasing w, the intensity variation is linear and finally reaches the same kinematical limit I_∞ as in the case of large strains without ultrasound.

The most interesting phenomenon is connected with the possible interference of X-ray trajectories. As has been noted, state 4 may be reached from point 1 by two trajectories: 1-2-6-7-3-4 (a) and 1-2-3-4 (b). Due to the conservation laws the final states corresponding to the zero-phonon process (b) and the process with phonon absorption and emission (a) are identical. Trajectories (a) and (b) meet at a point inside the crystal (see Fig. 1b) which is determined by the strain gradient b and the ultrasound frequency ν. Interference between the amplitudes of the two scattering processes leads to the oscillating dependence (of order B^{-1} at the fixed ν value) of the diffraction intensity. These oscillations modify the expression (3) as follows:

$$\Delta I/I_d = -2R_1M_1(1-\cos 2\varphi) \qquad (8)$$

with phase factor (Iolin, Raitman, Kuvaldin & Zolotoyabko, 1988)

$$2\varphi = (\Omega/B)(\Omega^2-1)^{1/2}; \quad \Omega = k/\Delta k_0. \qquad (9)$$

From the physical point of view it is clear that the mechanism of the anomalous behavior of diffraction intensity and trajectories interference 'operates' only if the strain gradient b exceeds some threshold value b_{th}. Actually, the atomic-plane curvature R^{-1} (for pure cylindrical bending $R^{-1} = b$) should be enough to close the quanta trajectories (Fig. 1b) within the limits of the crystal thickness T. It can be shown (Iolin, Raitman, Kuvaldin & Zolotoyabko, 1988) that

$$B_{th} = (2/\Delta k_0 T)(\Omega^2-1)^{1/2}. \qquad (10)$$

Note that interference of the X-ray wave fields corresponding to the different DS branches leads to the usual *Pendellösung* effect in perfect crystals. Less trivial is the partial conservation of the wave field coherence in elastically deformed crystals (Kato, 1964; Hart, 1966). This coherence reveals itself again in the form of *Pendellösung* fringes, but with contraction of the fringe period (Hart, 1966; Kato & Ando, 1966). Such interference takes place (if the incident-beam width is sufficient) in spite of the wave vectors of X-ray quanta, moving along different paths, not being parallel at the meeting point (Fig. 1b). The use of ultrasound excitation of the strained crystal to some extent changes the situation. The deformation gradient serves again for the creation of crossing trajectories, but ultrasound-induced interbranch transitions result in completely identical states of

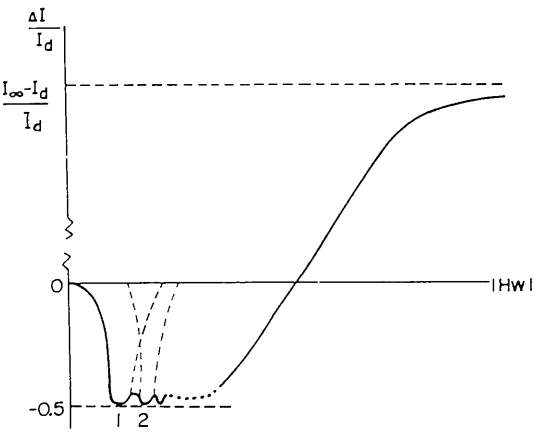

Fig. 2. Calculated relative variation of diffraction intensity $\Delta I/I_d$ depending on the sound amplitude w. Broken lines represent the contributions of multiphonon processes ($m = 1, 2, \ldots$) for small w. Parameter I_∞ gives the kinematical limit.

X-ray quanta at the meeting point (the wave vectors are equal and parallel). Hence, apart from the Kato interference in such a system, an additional interference process will exist, namely the interference of the above-mentioned trajectories (*a*) and (*b*), leading to the oscillating behavior of the diffraction intensity (under ultrasonic excitation), determined by the combination of strain gradient and sound frequency.

3. Experimental data

The measurements were carried out with an Si(111) single-crystal wafer of diameter 3 in and $T \simeq 366$ μm. The sample was arranged on the X-ray diffractometer in the symmetrical Laue position. The reflections $6\bar{6}0$, $8\bar{8}0$ were used with Mo $K\alpha$ radiation. The transverse acoustic waves with the wave vector $\mathbf{k} \| [111]$ and polarization vector $\mathbf{e} \| [2\bar{2}0]$ were excited by means of a quartz piezocrystal (Y cut, 10×15 mm, with the fundamental harmonic $\nu_0 = 18.8$ MHz), which was attached to the silicon with epoxy resin. The selection of sound frequency was done as follows.

The dependence of the diffraction intensity on sound frequency was measured for an unstrained crystal. In Fig. 3 an example of such a resonant diffraction spectrum for reflection $6\bar{6}0$ is shown. The intensity peaks correspond to the excitation of the self-shear vibrations of the Si wafer (standing waves), which obey the standard condition

$$nc/2\nu = T \qquad (11)$$

where c is the sound velocity and n is the harmonic number. Thus the silicon wafer operates as an additional filter which selects from the quartz resonance line (around $\nu = 3\nu_0$) the frequencies in accordance with expression (11). In fact, the harmonics with $n = 7, 8, 9$ are seen in Fig. 3.

Since we are interested in high-frequency ultrasound [condition (1)], it is necessary to know the threshold frequencies ν_{th}, corresponding to the equality $k = \Delta k_0$:

$$\nu_{th} = c/\tau. \qquad (12)$$

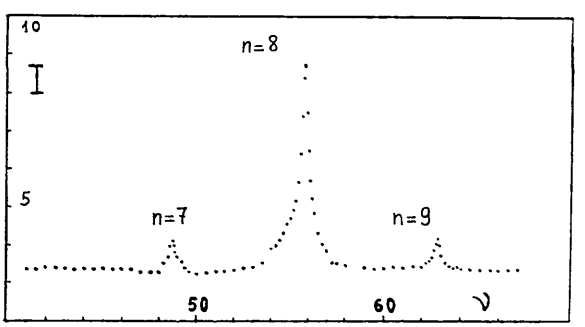

Fig. 3. Reflection $6\bar{6}0$. The resonant X-ray diffraction spectrum I (arbitrary units), depending on sound frequency ν (MHz).

Table 1. *The values of extinction length τ and threshold frequency ν_{th} for* Si(*hh*0) *reflections*

Mo Kα, σ polarization.

hkl	τ (μm)	ν_{th} (MHz)
220	36.6	139.3
440	54.2	94.1
660	88.8	57.4
880	133.8	38.1

The ν_{th} values, as well as the extinction lengths τ, calculated for Si(*hh*0) reflections with the aid of Si structure factors (Teworte & Bonse, 1984) are summarized in Table 1.

Elastic strain on the crystal wafer was provided by means of a simple bending device, which is schematically represented in the insert of Fig. 4. This method is not very suitable for measurements in Laue geometry (Okkerse & Penning, 1963; Hart, 1965) since it leads mainly to the bending of atomic planes parallel to the wafer faces [(111) in our case]. Nevertheless, as can be seen from our experiments, the distortion of the perpendicular 'working' planes of the type $(2\bar{2}0)$ is sufficient to create visible variations of diffraction intensity.

For strain calibration the magnitudes of the diffraction intensity without ultrasound excitation were used. Consider first the results obtained for the $6\bar{6}0$ reflection near the threshold frequency, when the ninth Si harmonic ($\nu = 62.55 \geq \nu_{th} = 57.4$ MHz) was used.

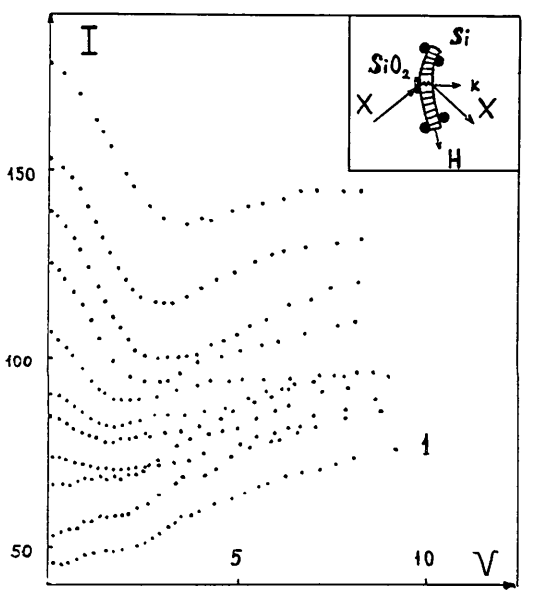

Fig. 4. Dependence of diffraction intensity I (10^3 counts/10 s) on sound amplitude $w \simeq V$ for the reflection $6\bar{6}0$ and $\nu = 62.45$ MHz. Curve 1 corresponds to the unstrained sample. In the upper right corner the experimental scheme is represented.

3(*a*) *The case* $\nu \geq \nu_{th}$

In the experiment the dependence of the diffraction intensity I on the sound amplitude w for different elastic strains was measured. The appropriate part of the experimental curves is shown in Fig. 4. The sound amplitude w is proportional to the voltage V applied to the piezocrystal. The higher the curve, the greater the wafer bends and correspondingly the greater the strain value. The formation of the anomalous shape of the $I(w)$ curves (with the decrease of diffraction intensity at small sound amplitudes) is clearly seen, starting from some threshold strain gradient value. Only initial regions of the curves (under weak ultrasonic excitation) are represented in Fig. 4. Measurements at strong acoustic field give the proof of identity of experimental and theoretical curves (Fig. 2) right up to the kinematical limit. Note that the situation near the threshold frequency is very 'sensitive' to elastic strains. The B_{th} value is very low [see (10)]: $B_{\text{th}} = 0.033$; it corresponds to a curvature radius of the $(2\bar{2}0)$ planes of $R = 1.2$ km in the model of cylindrical bending when

$$R = b^{-1} = H\tau^2/2\pi^2 B. \tag{13}$$

Further, from Fig. 4 we see that the position of the $I(w)$ minimum depends on the B value. With B increasing, the position V_{min} shifts to the right. Rewriting (3) [using (4)] in the form

$$\Delta I/I_d = -2\exp(-\alpha V/B^{1/2})[1-\exp(-\alpha V/B^{1/2})], \tag{14}$$

where α is an empirical coefficient, describing the relation between sound amplitude w and electrical voltage V and differentiating with respect to the parameter V, one obtains

$$B = (\alpha^2/\ln^2 2)\, V_{\text{min}}^2. \tag{15}$$

The square of V_{min} is linearly proportional to the B value. In Fig. 5 such a dependence, obtained by the treatment of $I(V)$ curves, is represented. The strain gradient was derived from the starting diffraction intensities $I_d = I(0)$ (without ultrasound) by means of the expression (see, for example, Iolin, Raitman, Kuvaldin & Zolotoyabko, 1988)

$$I_d/I_0 = 4BT/\tau. \tag{16}$$

For the parameter I_0, the magnitude $I(0)$ for curve 1 in Fig. 4, measured for an unstrained crystal, was used. The experimental points in Fig. 5 are in good agreement with the linear law, except in the region of low strain, where (16) is not valid. After preliminary checking of the experimental data, a search can begin for oscillations due to the possible interference trajectories.

According to (8), the intensity oscillations must occur at each sound amplitude, changing either the strain gradient or parameter Ω, depending on sound frequency (9). However, from the experimental point of view it is convenient to choose the 'sound effect' $\eta = \Delta I/I_d$ at the minimum point of $I(V)$ and to observe its variation under crystal deformation. The curve $\eta(B^{-1})$ obtained using this treatment (Fig. 4) is shown in Fig. 6. The starting B values were again chosen with the aid of (16).

Note, firstly, that the magnitude of the parameter η never reaches the predicted value of 50%. It seems that the reason is connected with the theoretical description in § 2, which strictly speaking was developed for neutron propagation. For X-rays, the time averaging on the standing-wave period must be undertaken and such a procedure will lead to a decrease of the observable η values.

The arrows in Fig. 6 show the positions of the first η maximum and minimum, calculated by means of

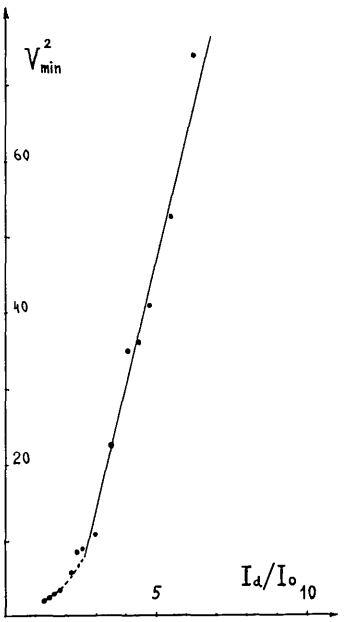

Fig. 5. The square of the minimum positions V^2_{min} of the $I(V)$ curves, depending on the strain gradient $b \simeq I_d/I_0$.

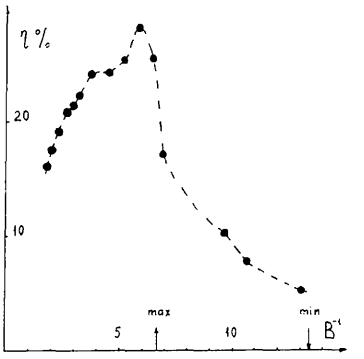

Fig. 6. Dependence of the sound effect $\eta = \Delta I/I_d$ [at the minimum point of $I(V)$] on the reduced reciprocal strain gradient B^{-1}. Si(6$\bar{6}$0), $\nu = 62.55$ MHz.

(8) and (9). Although the overall curve behavior is quite reasonable, it does not give a convincing proof of the oscillation pattern. The situation near the threshold frequency is not favorable for the oscillation display, since the period $\Delta(B^{-1})$ between maxima and minima

$$\Delta(B^{-1}) = \pi/[\Omega(\Omega^2-1)^{1/2}] \qquad (17)$$

is too large when Ω tends to 1. To obtain more reliable data it is necessary to go away from the threshold frequency to the region of $\nu > \nu_{\text{th}}$.

3(*b*) *The case* $\nu > \nu_{th}$

This regime can be realized in two ways: firstly, by means of a simple increase of the 'work' frequency ν at given ν_{th} or, secondly, by the variation of ν_{th} at fixed ν. The measurements were completed for both of these. The results for reflection $6\bar{6}0$, *i.e.* for $\nu_{\text{th}} =$ 57.4 MHz, are given below.

Measurements were carried out in the same manner as was described in the previous paragraph, but using the sound frequency $\nu = 90.45$ MHz. This corresponds to the fifth quartz harmonic and $n = 13$ harmonic of the silicon wafer. The dependence of the diffraction intensity I on the sound amplitude $w \simeq V$ was measured at different elastic strains. For each curve the sound effect $\eta = \Delta I / I_d$ was determined at the minimum point of the diffraction intensity. These data, depending on the B^{-1} values, are shown in Fig. 7. The arrows correspond to the extreme positions, calculated with (8) and (9). At least two oscillations are clearly seen in Fig. 7. Since $B_{\text{th}}^{-1} = 10.6$ [see (10)], only the part of these data obtained for $B^{-1} < B_{\text{th}}^{-1}$ can be rigorously treated in the framework of the above-mentioned theoretical considerations. Such a B_{th} value corresponds to the curvature radius of the $(2\bar{2}0)$ planes of $R = 415$ m.

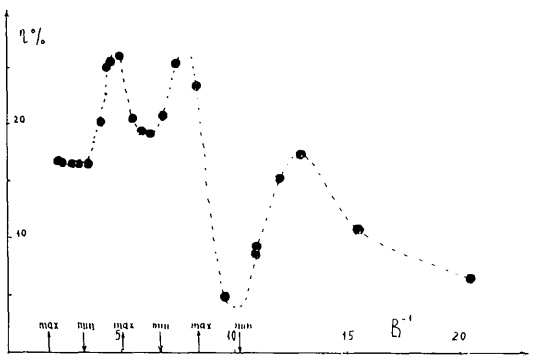

Fig. 7. The same data as that in Fig. 6, except $\nu = 90.45$ MHz.

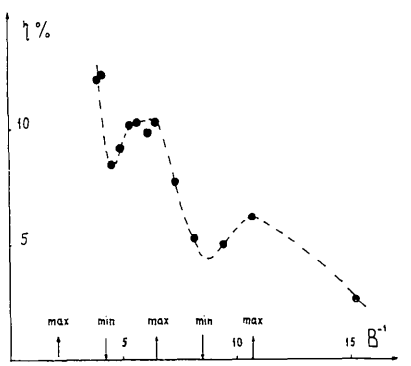

Fig. 8. The same data as that in Fig. 6, except for Si reflections $(8\bar{8}0)$ and $\nu = 54.71$ MHz.

At fixed X-ray wavelength we have a single possibility to change the threshold frequency ν_{th} using another crystal reflection *hkl* [see (12)]. Consider the data for $hkl = 8\bar{8}0$, which were obtained with the frequency $\nu = 54.71 > \nu_{\text{th}} = 38.1$ MHz (see Table 1). This frequency corresponds to the third quartz harmonic and $n = 8$ harmonic of the silicon wafer. The sound effect η depending on the reciprocal strain gradient B^{-1} [reduced value, according to (2)] is shown in Fig. 8. The threshold value $B_{\text{th}}^{-1} = 8.3$ corresponds to $R = 988$ m. Again, in the region where the theory is valid ($B^{-1} < B_{\text{th}}^{-1}$), there is a qualitative agreement of experimental data with the calculated positions (arrows) of the maxima and minima.

4. Concluding remarks

The study of X-ray diffraction in an elastically strained crystal under ultrasonic excitation has been undertaken. The results obtained give proof of the fine details of the quantum-mechanical behavior of X-rays inside a bent crystal. Using the combination of elastic strain and high-frequency ultrasound, we can construct two different X-ray trajectories, which meet inside the sample and provide at the meeting place identical quantum conditions for X-rays. As a result, a new kind of oscillation in diffraction intensity arises, depending on the reciprocal strain gradient b^{-1} and the sound frequency.

Apart from the fundamental aspect, such a new *Pendellösung* effect can in principle be used to measure the elastic strains and curvature of atomic planes in single crystals.

Measurements were carried out in the Physics Institute of the Latvian Academy of Sciences (Riga, Latvia, USSR) and we would like to thank colleagues from the laboratory of nuclear methods for technical assistance and, especially, Professor E. Iolin for helpful discussions.

References

CHUKHOVSKII, F. & PETRASHEN, P. (1977). *Acta Cryst.* **A33**, 311-319.

ENTIN, I. (1977). *Sov. Phys. JETP Lett.* **26**, 269-271.

ENTIN, I. (1979). *Sov. Phys. JETP*, **50**, 110-113.

ENTIN, I. & PUCHKOVA, I. (1984). *Sov. Phys. Solid State*, **26**, 1995-1998.

HART, M. (1965). *Appl. Phys. Lett.* **7**, 96-98.
HART, M. (1966). *Z. Phys.* **189**, 269-291.
IOLIN, E. (1987). Preprint LAFI-102. Physics Institute of the Latvian Academy of Sciences, Salaspils, USSR.
IOLIN, E. & ENTIN, I. (1983). *Sov. Phys. JETP*, **58**, 985-989.
IOLIN, E., RAITMAN, E., KUVALDIN, B. & ZOLOTOYABKO, E. (1988). *Sov. Phys. JETP*, **67**, 989-997.
IOLIN, E., ZOLOTOYABKO, E., RAITMAN, E. & KUVALDIN, B. (1989). In Twelfth Eur. Crystallogr. Meet., Moscow. Collected Abstr., Vol. 3, p. 54.
IOLIN, E., ZOLOTOYABKO, E., RAITMAN, E., KUVALDIN, B. & GAVRILOV, V. (1986). *Sov. Phys. JETP*, **64**, 1267-1271.
KATO, N. (1964). *J. Phys. Soc. Jpn*, **19**, 67-77.
KATO, N. & ANDO, Y. (1966). *J. Phys. Soc. Jpn*, **21**, 964-968.
KOHLER, R., MOHLING, W. & PEIBST, H. (1974). *Phys. Status Solidi B*, **61**, 173-180.
LUKAS, P. & KULDA, J. (1989). *Phys. Status Solidi B*, **156**, 41-48.
OKKERSE, B. & PENNING, P. (1963). *Philips Res. Rep.* **18**, 82-94.
PENNING, P. & POLDER, D. (1961). *Philips Res. Rep.* **16**, 419-440.
TEWORTE, R. & BONSE, U. (1984). *Phys. Rev. B*, **29**, 2102-2108.

Acta Cryst. (1992). A**48**, 231-236

Band-Structure Calculations and Structure-Factor Estimates of Cu – their Complementarity

BY J. K. MACKENZIE

Division of Materials Science and Technology, CSIRO, Clayton, Victoria, Australia 3168

AND A. MCL. MATHIESON

Division of Materials Science and Technology, CSIRO, Clayton, Victoria, Australia 3168 *and Chemistry Department, La Trobe University, Bundoora, Victoria, Australia* 3083

(*Received* 4 *February* 1991; *accepted* 17 *September* 1991)

Abstract

Rather than an uncritical comparison of experimental and theoretical values, the various sets of structure-factor values of copper metal derived from experimental diffraction procedures are mutally compared as also are the various sets of theoretical values derived from band-structure calculations. This approach reveals the presence of outlier sets in each group and allows recognition of their condition before any attempt is made to intercompare the groups. Within the experimental group, the γ-ray values do not appear to sustain the absolute status originally claimed for them. Within the theoretical group, an inadequacy in defining the core contribution is indicated. The latter conclusion suggests that it is an inappropriate operation to make direct comparison between diffraction-sourced experimental values of structure factors and theoretical values from band-structure calculations. Instead, the latter should be used on a *complementary* basis with the full $(\sin\theta)/\lambda$ range of experimental values to establish the best core contribution. The minor valence-bond contribution to scattering, which is largely restricted to the low $(\sin\theta)/\lambda$ region, is most sensitively defined by reference to band-structure prediction of photoemission spectral distribution. Attention is drawn to the possible significance of the form-factor curve *versus* $(\sin\theta)/\lambda$ being dependent on the unit-cell dimension.

Introduction

When there are many published sets of structure-factor values which have been determined by various experimental means and also those derived by theoretical calculations, comparison procedures to determine 'best' values require careful consideration. In many cases, experimental and theoretical values have been compared quite arbitrarily so that individual features intrinsic to experimental details or data reduction, on the one hand, or theoretical approximations and underlying assumptions, on the other, go unrecognized.

A more logical approach is to consider first the two groups separately. This provides a preliminary insight into each area, with respect to the spread of values, indications of consistency and trends with time. Only after such a procedure may it be appropriate to make a comparison between the two areas.

Indeed it becomes obvious on applying this approach to the published evidence for Cu that even a direct comparison of the two areas may not be wholly appropriate. Rather, from consideration of the bases of the numerical results from the two sources, it appears more likely that band-structure calculations and structure-factor values from diffraction techniques provide *complementary* (rather than comparable) views of the details of the total charge-density distributions in solids.

0108-7673/92/020231-06$03.00